Available online at www.sciencedirect.com
SCIENCE DIRECT®
Journal of Catalysis 213 (2003) 47–62
JOURNAL OF CATALYSIS
www.elsevier.com/locate/jcat

A comparison between silica-immobilized ruthenium(II) single sites and silica-supported ruthenium nanoparticles in the catalytic hydrogenation of model hetero- and polyaromatics contained in raw oil materials

Claudio Bianchini,[a,*] Vladimiro Dal Santo,[b] Andrea Meli,[a] Simonetta Moneti,[a] Marta Moreno,[a] Werner Oberhauser,[a] Rinaldo Psaro,[b] Laura Sordelli,[b] and Francesco Vizza[a]

[a] *ICCOM-CNR, Via J. Nardi 39, 50132 Florence, Italy*
[b] *ISTM-CNR, Via C. Golgi 19, 20133 Milan, Italy*

Received 9 April 2002; revised 29 August 2002; accepted 3 September 2002

Abstract

A comparative study of the hydrogenation of various heterocycles, model compounds in raw oil materials, by either Ru(II) complex immobilized on mesoporous silica or Ru(0) nanoparticles deposited on the same support has been performed. The single-site catalyst contains the molecular precursor $[Ru(NCMe)_3(sulphos)](OSO_2CF_3)$ tethered to partially dehydroxylated high-surface-area silica through hydrogen bonds between silanol groups of the support and SO_3^- groups from both the sulphos ligand $[^-O_3S(C_6H_4)CH_2C(CH_2PPh_2)_3]$ and the triflate counter anion. Highly dispersed ruthenium nanoparticles were prepared by calcination/reduction of silica-supported $Ru_3(CO)_{12}$. The heterocycles (benzo[*b*]thiophene, quinoline, indole, acridine) are hydrogenated to cyclic thioethers or amines. The Ru(II) single-site catalyst is active for both benzo[*b*]thiophene and the *N*-heterocycles, while the Ru(0) catalyst does not hydrogenate the *S*-heterocycle, yet is efficient for the reduction of the *N*-heterocycles and simple aromatic hydrocarbons. The surface silanols promote the hydrogenation of indole via N–H···O(H)–Si≡ hydrogen bonds and can interact with the π-electron density of all substrates.

Keywords: Immobilized catalyst; Single-site catalyst; Mesoporous silica; Ruthenium; Hydrogen bonds; Hydrogenation of sulfur and nitrogen heterocycles

1. Introduction

Hydrodesulfurization (HDS) and hydrodenitrogenation (HDN) are very important hydrotreating reactions that serve to remove sulfur and nitrogen from fossil fuels where they are contained in various organic compounds, which include polyaromatic heterocycles, aliphatic and aromatic thiols and amines, thioethers, disulfides, and nitriles [1]. The aromatic heterocycles are the most difficult to degrade by hydrotreating [1–3].

Over the past 10 years, homogeneous modeling studies applying transition metal complexes have provided a huge amount of mechanistic information on the elementary steps involved in the HDS of thiophenes [4–7] as well as the HDN of *N*-heterocycles such as quinoline, pyridine, indole, pyrrole, and acridine [4f,7b,8]. In the homogeneous modeling studies, however, the catalysts employed and the reaction conditions are remarkably different from those used in refinery reactors. Besides using spectator ligands that are not representative of the pools of ligands available to industrial hydrotreating catalysts, homogeneous modeling studies are limited by the use of polar solvents that may compete with the heterocycle for coordination and reactivity and by the occurrence of undesired metal–metal interactions via either intermolecular contacts or formation of clusters and aggregates. Most of these limitations can be overcome by the use of molecular complexes tethered to solid supports in such a way as to minimize or even eliminate any contact between metal sites [9,10]. For this purpose, an ideal support material is silica [11–14]. Site isolation can be more carefully defined on silica than on a flexible polymer backbone, in fact. Moreover, silica has a rigid structure and does not swell in solvents; hence, it can be used at both high and low temperatures and at high pressures even in continuous-flow reactors. Last but not least, metal particles can be immobilized on the

* Corresponding author.
E-mail address: bianchin@fi.cnr.it (C. Bianchini).

0021-9517/03/$ – see front matter
PII: S0021-9517(02)00027-1

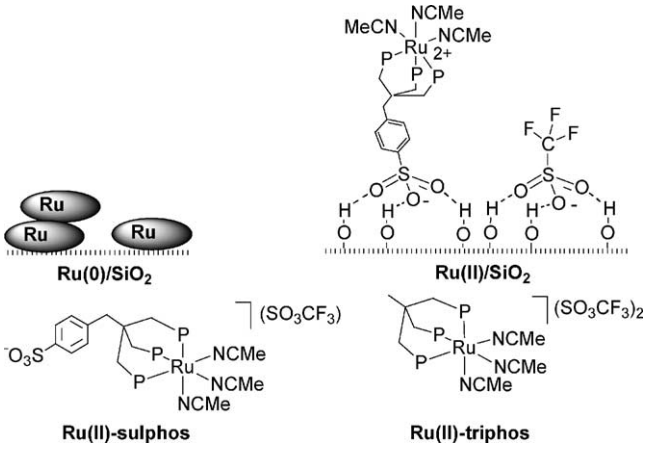

Chart 1.

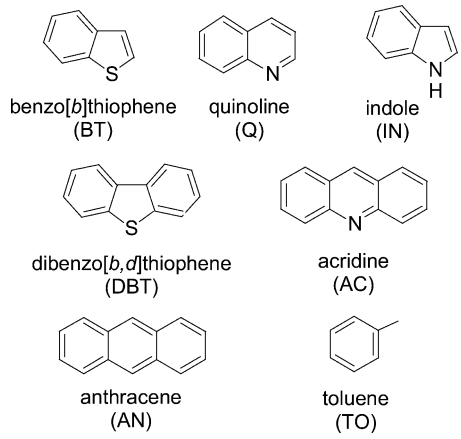

Chart 2.

silica surface by standard procedures, which allows one to compare the catalytic activity of single metal sites with that of contiguous metal sites.

This paper reports on the heterogeneous hydrogenation of various hetero- and polyaromatics by a molecular ruthenium(II) precursor immobilized on mesoporous silica. This catalyst, $[Ru(NCMe)_3(sulphos)](OSO_2CF_3)/SiO_2$ ($Ru(II)/SiO_2$), is shown in Chart 1; it has been previously prepared by immobilization of $[Ru(NCMe)_3(sulphos)](OSO_2CF_3)$ (Ru(II)-sulphos) on partially dehydroxylated high-surface-area silica through a linker which is sufficiently flexible and long to preserve the stereochemical properties of the parent homogeneous catalyst and to minimize steric interactions with the support surface [13]. The grafting modes of both complex cation and counteranion involve a hydrogen-bonding interaction between silanol groups of the support and SO_3^- groups from both the sulphos ligand $[^-O_3S(C_6H_4)CH_2C(CH_2PPh_2)_3]$ and the triflate anion [13,14].

To remove any ambiguity on the grafting mode of the ruthenium complex to silica, both $Ru(II)/SiO_2$ and Ru(II)-sulphos were studied by EXAFS methods [13c]. An EXAFS study has also been carried out on $Ru(0)/SiO_2$ that contains highly dispersed ruthenium nanoparticles obtained from $Ru_3(CO)_{12}$. In fact, central to our investigation is also a comparison between the silica-tethered Ru(II)-sulphos catalyst and the silica-supported Ru(0) nanoparticles [12n–t], but related homogeneous and aqueous-biphase systems have been considered when useful. All the catalysts employed in this study are shown in Chart 1.

Ruthenium has been chosen for its great potential in HDS/HDN catalysis [1a,b,7,15], while the substrates investigated are representative of the pool of compounds contained in raw oil materials (Chart 2).

2. Experimental

All reactions and manipulations were routinely performed under a nitrogen or argon atmosphere using standard Schlenk techniques. CH_2Cl_2 was distilled under nitrogen from CaH_2. THF, *n*-heptane, and *n*-octane were distilled under nitrogen from $LiAlH_4$. Deuterated solvents for NMR measurements (Merck, Aldrich) were dried over molecular sieves. Quinoline used in infrared studies was distilled in vacuo and stored under argon. The Davison 62 (Grace) silica employed in this work was a high-surface-area hydrophilic mesoporous material. The support was ground, washed with 1M HNO_3 and distilled water to neutrality, and dried overnight in an oven at 100 °C. Nitrogen adsorption/desorption isotherms at liquid nitrogen temperature were measured on a Micromeritics ASAP 2010 instrument. The samples were routinely preoutgassed at 300 °C, in the case of $Ru(II)/SiO_2$ the temperature chosen was 150 °C. Pore diameter and specific pore volume were calculated according to the Barret–Joyner–Halenda (BJH) theory [16]. The specific surface area was obtained using the Brunauer–Emmett–Teller (BET) equation [17]. All the other reagents and chemicals were reagent grade and were used as received from commercial suppliers. The silica-tethered ruthenium complex $Ru(II)/SiO_2$ (ca. 1.7 wt% Ru) [13b] and the soluble derivatives Ru(II)-sulphos [13b] and $[Ru(NCMe)_3(triphos)](OSO_2CF_3)_2$ [18] (Ru(II)-triphos) were prepared as previously described [triphos = $MeC(CH_2PPh_2)_3$]. $Ru_3(CO)_{12}$ was synthesized from $RuCl_3 \cdot xH_2O$ (Engelhard) following a procedure reported in the literature [19]. Batch reactions under a controlled pressure of gas were performed with a stainless steel Parr 4565 reactor (100 ml) equipped with a Parr 4842 temperature and pressure controller and a paddle stirrer. The ruthenium contents in the tethered catalysts were determined by inductively coupled plasma atomic emission spectroscopy (ICP-AES) with a Jobin Yvon (series JY24) instrument at a sensitivity level of 500 ppb. Each sample (20–50 mg) was treated in a microwave-heated digestion bomb (Milestone, MLS-200) with concentrated HNO_3 (1.5 ml), 98% H_2SO_4 (2 ml), 37% HCl (0.5 ml), and a pellet (0.5 g) of a digestion aid reagent (0.1% Se in K_2SO_4). After the silica particles were filtered off, the solutions were analyzed. The

addition of selenium was necessary to get effective digestion of the phosphine ligand, which was hardly achievable by the usual acid dissolution procedures. The same digestion method was employed to determine the metal contents in the products recovered after catalysis as well as the organic solutions. Like the tethered catalysts, the ruthenium contents in the heterogeneous catalyst $Ru(0)/SiO_2$ were determined by ICP-AES with the same Jobin Yvon instrument. However, each sample (ca. 50 mg) was treated with a mixture of 4 ml of a NaOCl solution (6–14% free chlorine Riedel–de Haën) and 2 ml of 2 M NaOH and heated to boiling temperature for a few minutes. The resulting solutions were analyzed after bringing the volume to 50 ml in a volumetric flask. ^1H (200.13 MHz) and $^{31}P\{^1H\}$ (81.01 MHz) NMR spectra were obtained on a Bruker ACP 200 spectrometer. Chemical shifts (δ) are reported in ppm relative to tetramethylsilane referenced to the chemical shifts of residual solvent resonances (^1H) or 85% H_3PO_4 (^{31}P) with downfield values reported as positive. Solid-state ^{31}P NMR spectra were recorded on a Bruker AMX 300 WB spectrometer equipped with a 4-mm BB-CP MAS probe at a working frequency of 121.50 MHz. Further details relative to the acquisition and processing of the CP MAS spectra have been reported elsewhere [13b,c]. High-pressure NMR (HPNMR) experiments were carried out in 10-mm sapphire tubes. These were purchased from Saphikon, Milford, NH, while the titanium high-pressure charging head was constructed at the ISSECC-CNR (Florence, Italy) [20].[1] GC analyses of the solutions were performed on a Shimadzu GC-14A gas chromatograph equipped with a flame ionization detector and a 30-m (0.25 mm i.d., 0.25 μm film thickness) SPB-1 Supelco fused silica capillary column. GC/MS analyses were performed on a Shimadzu QP 5000 apparatus equipped with an identical capillary column.

2.1. IR and DRIFT spectra

These spectra were recorded on a Digilab FTS-60 equipped with a KBr beam-splitter and a DTGS detector operating between 400 and 4000 cm^{-1}. Transmission spectra were recorded on wafers obtained by pressing in air the silica powder, pretreated at 500 °C and hydrated as previously described [13b], at 2 ton cm^{-2} (18 mm in diameter, 50 mg). The wafers were placed in a specially designed T-shaped Pyrex cell equipped with CaF_2 windows. This cell makes it possible to carry out thermal treatments as well as to operate in a vacuum or under a controlled atmosphere. The silica wafers were treated at 300 °C in air for 3 h, maintained under vacuum (10^{-5} mbar) overnight at the same temperature, impregnated in situ under argon with anhydrous *n*-heptane solutions of heterocyclic compounds, and finally dried under vacuum (10^{-3} mbar) just to disappearance of the IR absorption bands characteristic of the solvent. The technique of both impregnation and workup to obtain IR spectra of supported organometallic compounds in the complete absence of air and moisture has been described elsewhere [21]. DRIFT spectra of $Ru(0)/SiO_2$ and $Ru(II)/SiO_2$ were recorded using a Harrick reaction chamber with KBr windows and Harrick DRA-2C1 accessory. The catalysts were placed in the cell sample holder under inert atmosphere. The cell was connected to a vacuum gas line for the sample treatment and to a programmable heater operating from ambient temperature to 450 °C. Samples of $Ru(0)/SiO_2$ were obtained by calcinating and reducing *in situ* $Ru_3(CO)_{12}/SiO_2$ under the same conditions as reported for the preparation of the samples used in catalytic experiments (see below).

2.2. Preparation of $Ru(0)/SiO_2$

A solution of $Ru_3(CO)_{12}$ (200 mg) in 60 ml of anhydrous CH_2Cl_2 was added to pretreated silica (ca. 5.0 g) under argon. The resulting mixture was stirred for 5 h at room temperature. After all the solvent was evaporated under vacuum (10^{-3} mbar), the solid $Ru_3(CO)_{12}/SiO_2$ residue was dried overnight under vacuum (10^{-3} mbar) at room temperature. Samples of the supported ruthenium cluster (ca. 0.5 g) were maintained in oxygen flow at 200 °C for 1 h (heating ramp 10 °C min^{-1}). After cooling to room temperature in a flow of argon, each sample was reduced in hydrogen flow at 220 °C for 1 h (heating ramp 10 °C min^{-1}) and then cooled to room temperature under argon. This procedure allowed the reproducible preparation of samples containing ruthenium at ca. 1.7 wt%.

2.3. HRTEM measurements

A $Ru(0)/SiO_2$ sample (10 mg) was ground and the resulting powder was ultrasonically dispersed in *n*-heptane (10 ml). Drops of the resulting suspension were deposited on holey carbon grids that, after evaporation of the solvent, were introduced into the sample compartment of a JEOL100 high-resolution transmission electron microscope. Micrographs of the sample were taken at × 340,000 magnification.

2.4. EXAFS experiments

X-ray absorption spectra were collected at the BM29 station at the ESRF (Grenoble, France) with a Si(311) double crystal monochromator. Harmonic rejection was achieved by a 50% detuning of the two Si crystals. Rhodium metal foil was used for the angle/energy calibration. Spectra were recorded at 27 °C in transmission mode, at the Ru *K*-edge over the range 21.8–23.3 keV, with an energy sampling step of 1 eV and an integration time of 2 s per point. Incident and transmitted photon fluxes were detected with ionization chambers filled with 1.1 bar of Ar and 0.3 bar of Kr, respectively. Each spectrum was acquired

[1] Since high gas pressures are involved, safety precautions must be taken at all stages of studies involving high-pressure NMR tubes.

three times. The unsupported complex Ru(II)-sulphos was ground up with boron nitride prior to recording the spectra to give a metal content of approximately 10%. The supported samples were loaded under inert atmosphere. Extracted $\chi(k)$ data were averaged before the EXAFS data analysis. Experimental $\chi(k)$ data were extracted from absorption data with the PAXAS program [22], whose procedure is outlined as follows: a polynomial background was fitted in the pre-edge region, extrapolated to higher energies, and then subtracted from absorption data. The atomic-like contribution was estimated by a polynomial fit and then subtracted from experimental data following the procedure proposed by Lengeler and Eisenberger [23]. The result was normalized to edge height to obtain experimental $\chi(k)$. The spherical wave curve-fitting analysis was performed by least-squares refinement of non-Fourier-filtered $\chi(k)$, using the EXCURVE program (developed by Gurman and Binsted) [24], using Van–Barth ground state potentials and Hedin–Lundquist exchange potentials. The k^3-weighted $\chi(k)$ data and their Fourier transformed spectra over a Kaiser window in the k range of 3–15 $Å^{-1}$ are reported in all plots, together with the corresponding theoretical best fits.

2.5. Heterogeneous hydrogenation reactions with Ru(0)/SiO_2

A 100-ml Parr autoclave was charged with Ru(0)/SiO_2 (1.7 wt% Ru, 130 mg, 2.2×10^{-2} mmol Ru), the desired amount of substrate, *n*-octane (30 ml), and H_2 (30 bar). The ensemble was heated to 100 °C and then stirred (1500 rpm) for 1 h, after which the vessel was cooled to ambient temperature and depressurized. The liquid contents were analyzed by GC and GC/MS. Above 1500 rpm, the rates were independent of the agitation speed at all the temperatures studied, thus indicating the absence of mass transport limitations.

2.6. Heterogeneous hydrogenation reactions with Ru(II)/SiO_2

A 100-ml Parr autoclave was charged with Ru(II)/SiO_2 (1.7 wt% Ru, 130 mg, 2.2×10^{-2} mmol Ru), the desired amount of substrate, *n*-octane (30 ml), and H_2 (30 bar). The ensemble was heated to 100 °C and then stirred (1500 rpm) for the desired time, after which the vessel was cooled to ambient temperature and depressurized. The liquid contents were analyzed by GC and GC/MS. Above 1500 rpm, the rates were independent of the agitation speed at all the temperatures studied, thus indicating the absence of mass transport limitations. The stability of the immobilized catalyst against leaching from the support was tested as follows:

(i) After a catalytic run, the grafted ruthenium product was separated by filtration from the liquid phase under nitrogen, washed with *n*-octane, and then reused for a second, identical run. After the liquid phase was analyzed by GC, the solvent was removed under vacuum and the residue was analyzed by both $^{31}P\{^1H\}$ NMR spectroscopy and ICP-AES. No trace of phosphorus was seen by NMR spectroscopy in all cases, while the amounts of ruthenium detected by ICP-AES were < 1 ppm. A similar loss of ruthenium was generally determined in the tethered termination products.

(ii) In order to refrain from filtering the solid catalyst after each catalytic run, several reactions were carried out in a 100-ml Parr reactor fitted with a dip pipe with a sintered (2 μm) metal piece at its dipping end. Upon termination of the reaction, the solution was forced out through the sintered dip pipe by applying a nitrogen pressure of ca. 2 bar at the gas inlet valve of the reactor, thus retaining the catalyst in the reactor under nitrogen. The catalyst was washed with *n*-octane (3×20 ml). After a sample of the filtrate was analyzed by GC, most of the solvent was distilled out and the residue was analyzed by ICP-AES. A fresh *n*-octane solution of the substrate to be hydrogenated was then loaded through a thin Teflon pipe connected to the reactor. The reactor was then pressurized with hydrogen to 30 bar, heated to the appropriate temperature and then stirred for the desired time.

In separate experiments, finely crushed Ru(II)-sulphos or Ru(II)-triphos was used as catalyst precursor in the place of the supported species Ru(II)/SiO_2. Irrespective of the substrate, no hydrogenation was observed under comparable reaction conditions.

2.7. Homogeneous hydrogenation reactions with Ru(II)-triphos

As a general procedure, a 100-ml Parr autoclave was charged with Ru(II)-triphos (25 mg, 2.2×10^{-2} mmol), the unsaturated substrate, THF or CH_2Cl_2 (30 ml), and H_2 (30 bar). The ensemble was heated to 100 °C and then stirred (750 rpm) for the desired time. After the vessel was cooled to ambient temperature and depressurized, the liquid contents were analyzed by GC and GC/MS. In selected runs, the final reaction mixture was concentrated to dryness *in vacuo* and the residue, dissolved in an appropriate deuterated solvent, was analyzed by NMR spectroscopy.

2.8. Aqueous-biphase hydrogenation reactions with Ru(II)-sulphos

A 100-ml Parr autoclave was charged with Ru(II)-sulphos (25 mg, 2.2×10^{-2} mmol), the unsaturated substrate, *n*-octane (15 ml), water (15 ml), and H_2 (30 bar). The ensemble was heated to 100 °C and then stirred (1500 rpm) for the desired time, after which the vessel was cooled to ambient temperature and depressurized. As a general procedure, THF was added to the final catalytic mixtures

until a unique phase was observed, which was analyzed to obtain the total distribution of products. Above 1500 rpm, the rates were independent of the agitation speed at all the temperatures studied, thus indicating the absence of mass transfer resistance.

2.9. In situ NMR studies of hydrogenation reactions catalyzed by Ru(II)/SiO_2

In a typical HPNMR experiment, a 10-mm sapphire tube was charged with C_6D_6 (2 ml), Ru(II)/SiO_2 (1.7 wt% Ru, 100 mg, 1.7×10^{-2} mmol Ru), and a 20-fold excess of substrate (0.34 mmol) under nitrogen at room temperature. The tube was pressurized with hydrogen to 30 bar and then placed into a NMR probe at room temperature (ca. 10 min after pressurization). The temperature of the probe was then increased to 100 °C. As soon as the temperature was stabilized, ^{1}H and ^{31}P{^{1}H} NMR spectra were recorded every 5 min. After 1 h, the tube was cooled to room temperature and ^{1}H and ^{31}P{^{1}H} NMR spectra were acquired.

3. Results

3.1. Synthesis and characterization of the catalyst precursors

A highly dispersed Ru(0) metallic phase, free of any inorganic or organic residue, was obtained by calcination/reduction treatment of silica-supported $Ru_3(CO)_{12}$ under very mild conditions. Figure 1 shows the histogram of the metal particle size distribution for freshly prepared Ru(0)/SiO_2 as obtained by HRTEM. A uniform particle dispersion all over the support grains was obtained with a narrow distribution centered at about 1 nm, which is in good agreement with the value estimated from the EXAFS data (1.0–1.5 nm) (vide infra).

The size of the metal particles was less than the diameter of the silica mesopores, suggesting that the particles are also located inside the mesopores. No relevant decrease in the BET surface area and mesopore volume was observed, however (Table 1), which may be due to either very high dispersion of the ruthenium particles or low metal content.

Table 1
Surface area, pore volume, and average pore radius

	Surface area[a] ($m^2\,g^{-1}$)	Pore volume[b] ($cm^3\,g^{-1}$)	Av. pore radius[b] (nm)
SiO_2 (Davison 62)	344	1.19	5.83
Ru(0)/SiO_2	338	1.14	5.72
Ru(II)/SiO_2	272	0.80	4.94

[a] Calculated according to the BET method.
[b] According to the BJH theory.

The heterogenization of Ru(II)-sulphos was obtained following the solvent impregnation method previously described [13]. A nitrogen adsorption isotherm of the grafted complex showed a decrease of ca. 30% of the mesoporous pore volume compared to the corresponding silica carrier material (Table 1). The BET surface was found to decrease from 344 to 272 $m^2\,g^{-1}$ with a corresponding decrease in the pore volume from 1.19 to 0.80 $cm^3\,g^{-1}$. These results indicate that the molecular Ru(II) complex is anchored preferentially inside the pores of the support [25].

Three-gram samples of Ru(II)/SiO_2 with metal loadings of ca. 1.7 wt% were obtained in a reproducible way. Besides ruthenium analysis via ICP-AES, each sample was authenticated by comparing its ^{31}P CP-MAS NMR spectrum to that reported in the literature [13b].

An EXAFS analysis on Ru(II)/SiO_2 was carried out to look at possible interactions of the metal or its close environment with the silica surface. To better resolve the structure of the complex EXAFS signal, to which multiple shells and scattering contribute, the spectra of the unsupported parent complex Ru(II)-sulphos were analyzed first.

In Fig. 2 is reported a comparison between the Fourier spectra of free and silica-supported [Ru(sulphos)$(NCMe)_3$]-(SO_3CF_3), whose almost perfect overlap confirms that the complex cation is anchored intact on the support surface.

The results of the spherical wave curve-fitting analysis of the local surrounding of the absorbing atom, performed by

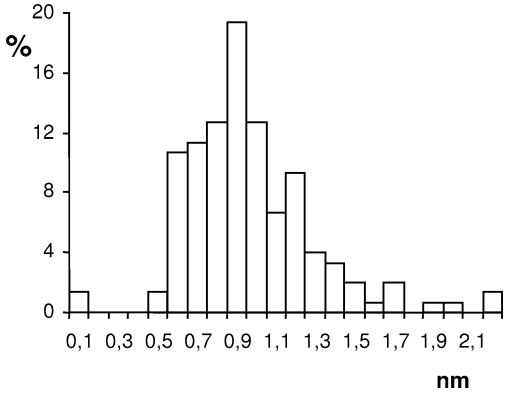

Fig. 1. Histogram of the Ru particle size distribution for Ru(0)/SiO_2 as measured by HRTEM micrographs.

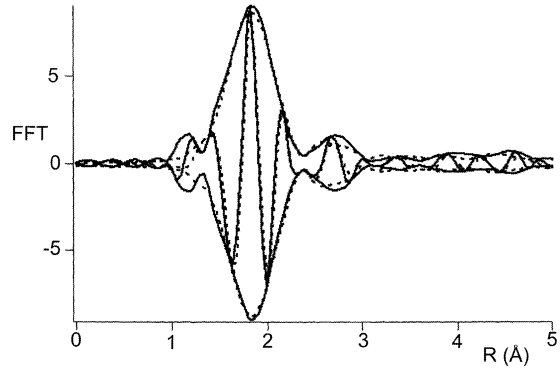

Fig. 2. Comparison of modulus and imaginary part of Ru K-edge k^3-weighted Fourier Transform spectra of Ru(II)-sulphos (—) and Ru(II)/SiO_2 (- - -).

Table 2
Curve-fitting results for the Ru K-edge EXAFS data

Sample	Shell	N	r (Å)	σ_{DW} (Å)
Ru(II)-sulphos	N	3.1 ± 0.1	2.083 ± 0.008	0.087 ± 0.006
	P	3.1 ± 0.1	2.316 ± 0.003	0.060 ± 0.002
	C	3.0 ± 0.2	3.05 ± 0.01	0.078 ± 0.008
$Ru(II)/SiO_2$	N	3.1 ± 0.1	2.129 ± 0.003	0.076 ± 0.003
	P	2.9 ± 0.1	2.326 ± 0.002	0.070 ± 0.002
	C	3.0 ± 0.1	3.031 ± 0.007	0.077 ± 0.008
$Ru(0)/SiO_2$	Ru	5.9 ± 0.2	2.617 ± 0.001	0.071 ± 0.002
	Ru	2.8 ± 0.2	3.737 ± 0.003	0.082 ± 0.001
	Ru	5.6 ± 0.3	4.625 ± 0.002	0.078 ± 0.004
	Ru	5.2 ± 0.2	5.061 ± 0.003	0.089 ± 0.006

least-squares refinement, are reported in Table 2. The main peak in the spectrum of the unsupported complex is originated by the three nitrogen atoms from the NCMe ligands and by the three phosphorus atoms from the tripodal ligand (Fig. 2). The second peak comes from the three carbon atoms of the NCMe ligands. Notably, the Ru–N and Ru–P distances are almost coincident with those obtained from a single-crystal X-ray analysis of Ru(II)-sulphos $(2.099(6)_{av}$ and $2.312(1)_{av}$ Å, respectively) [13b]. Multiple scattering has been employed for the NC moieties bound to ruthenium, with a bond angle of 174° between the carbon and the nitrogen atoms (averaged value taken from the crystal structure data). The Ru–C distance detected by EXAFS is shorter than the crystallographic distance $(3.218(4)_{av}$ Å) by approximately 0.17 Å and reflects the imperfect equivalence of the three acetonitrile ligands in terms of both Ru–N distance and Ru–N–C angle (the standard Gaussian description of the radial pair distribution underestimates distances in the presence of high conformational disorder). No further shell contribution to the EXAFS signal was visible in the spectrum. The damping σ_{DW} factor for the carbon atoms belonging to the sulphos phenyl groups was high due to their thermal and conformational disorder, which prevented the detection of any signal at a distance higher than about 3.5 Å.

In the spectrum of the supported sample, similar in appearance to that of Ru(II)-sulphos (Figs. 2 and 3a), three shells of atoms were still detectable. Three equidistant NC units from the metal were observed as with three phosphorus atoms (Table 2). The bond lengths from ruthenium were slightly elongated (by approximately 0.05 Å for N and 0.01 Å for P), which is probably a consequence of the hydrogen-bond grafting of the metal complex to the silica surface. No additional contribution coming from surface atoms or adjacent metal complexes was detected. Analogously, no relevant distortion from the structure of the unsupported parent complex was observed.

Since the chemical environment in the vicinity of the metal center of $Ru(II)/SiO_2$ is almost identical to that of the unsupported complex, one may definitely conclude that the ruthenium complex is tethered to the surface OH

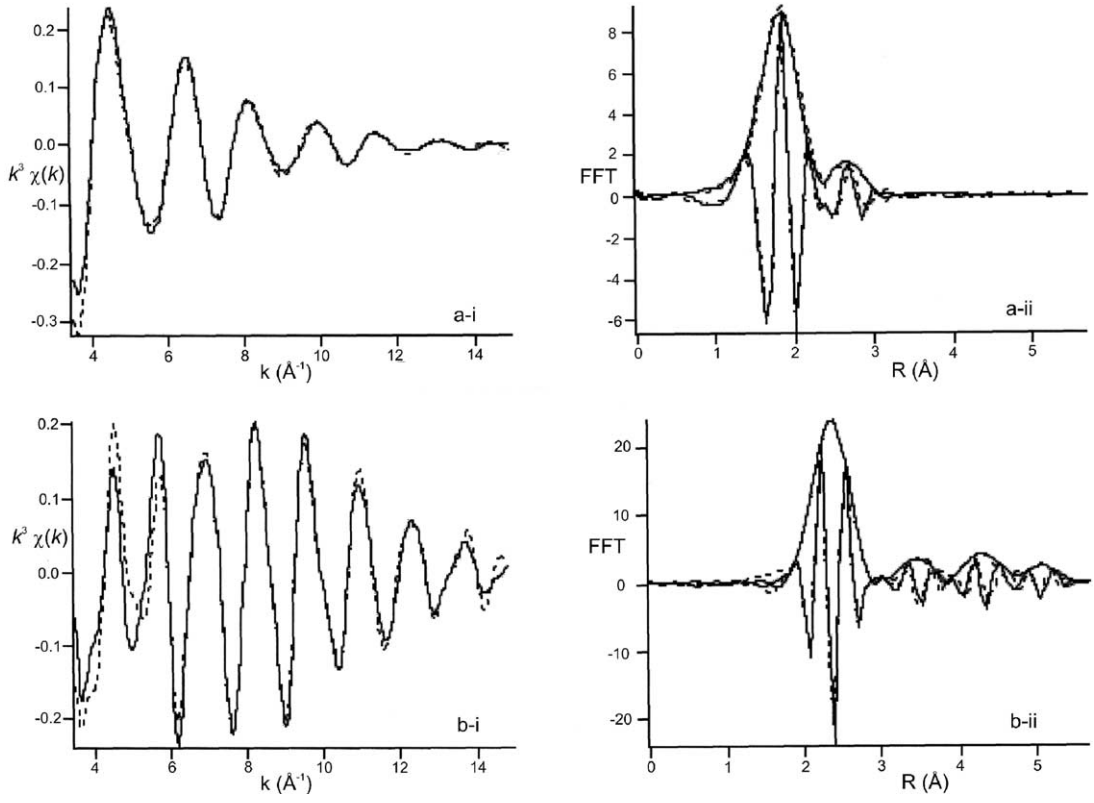

Fig. 3. Ru K-edge k^3-weighted EXAFS (i) and Fourier transform (ii) spectra of (a) $Ru(II)/SiO_2$; (b) $Ru(0)/SiO_2$; (- - -) experiment and (—) spherical wave theory.

groups through a linker that is sufficiently rigid to suppress metal–metal interactions, but also long enough to avoid any interaction with the support surface.

The Fourier spectrum of $Ru(0)/SiO_2$ contains four distinct peaks (Fig. 3b). The Ru–Ru neighbor numbers and distances (Table 2) are descriptive of the formation of small metal particles dispersed onto the support. As ruthenium metal has a close hexagonal crystal structure with 12 first neighbors at 2.677 Å, on the hypothesis that the supported particles have the same packing and had grown up with hemispherical geometry, the mean diameter corresponding to the value $N_1 = 5.9$ is 1.0–1.5 nm.

3.2. Interaction of silica with S- and N-heterocycles

The thermal pretreatment of the silica support employed in this work gave a material containing mostly isolated free silanols (Fig. 4, curve a) [13c]. However, for a loading of $Ru(II)/SiO_2$ of ca. 1.7 wt% metal, almost all isolated (3742 cm^{-1}) and vicinal (ca. 3690 cm^{-1}) silanols disappeared (Fig. 4, curve b) [13b]. Formed in their place were silanols in hydrogen interaction with the sulfonate groups from both metal complex cations and triflate ions, which gave a new broad adsorption band centered at ca. 3400 cm^{-1} [13b].

The procedure used to support the ruthenium particles to give $Ru(0)/SiO_2$ did not substantially modify the uncovered silica surface that still contained isolated and vicinal silanols (Fig. 4, curve c).

Five different types of model coal/petroleum heterocycles have been investigated in this work. All substrates interact with the silica surface using both the aromatic π-electron density ($\pi\cdots$H–O–Si≡ interactions) [26a–d] and the heteroatom [26e]. Benzo[*b*]thiophene (BT) and dibenzo[*b*, *d*]thiophene (DBT) bear a sulfur atom that only very strong electrophiles are able to attack [5], yet S···H–O–Si≡ bonds should contribute to adsorbing these substrates on the support. The *N*-heterocycles quinoline (Q; $pK_a = 4.9$) and acridine (AC; $pK_a = 5.6$) contain fairly basic nitrogen atoms [7b] that allow for the formation of N···H–O–Si≡ hydrogen bonds; in contrast, indole (IN) is not basic at all ($pK_a = -3.6$) and its nitrogen lone pair, being delocalized over the five-membered ring, is not available for interaction with electrophiles [27]. On the other hand, indole may form hydrogen bonds with the oxygen atom of either isolated or vicinal silanols (N–H···O(H)–Si≡) [26e]. Scheme 1 shows three out of the many possible hydrogen-bonding interactions of BT, Q, and IN with the silica surface.

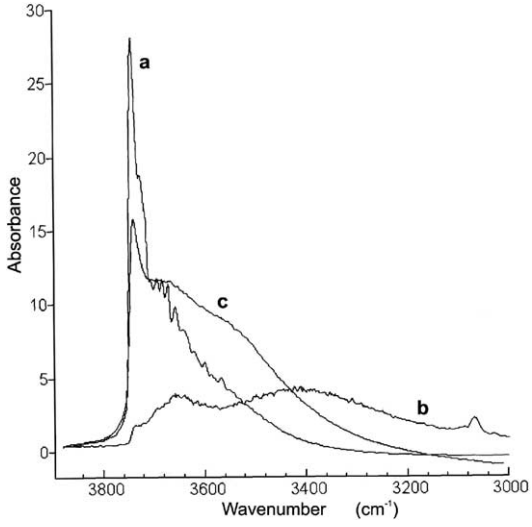

Fig. 4. DRIFT spectra in the ν(O–H) region of (a) pure SiO_2; (b) $Ru(II)/SiO_2$; (c) $Ru(0)/SiO_2$.

For technical reasons [28], it was not possible to get reliable IR data on the interaction between the various substrates and the surface of $Ru(II)/SiO_2$, yet fairly informative IR spectra in the O–H stretching region (Fig. 5) were obtained using pretreated-silica pellets containing comparable amounts of IN, Q, BT, and, for comparative purposes, *N*-methyl indole (MeIN). From a comparison with the IR spectrum of pure silica (trace a), one may readily realize that the contact between the various substrates and silica leads to a significant intensity decrease of the band due to the isolated silanols with a concomitant formation of a new band due to the silanols in hydrogen-bonding interaction with the π systems of the heterocycles [26a–d]. Interestingly, this band moves steadily to low frequency in the order Q (trace b) > BT (trace c) > MeIN (trace d) ≈ IN (trace e). IN apparently forms the greatest variety of hydrogen interactions, as shown by its covering the largest frequency range. The network of hydrogen interactions achievable by IN includes ≡Si–O–H···π(aromatic) and N–H···O(H)–Si≡ bonds as well as intermolecular N–H···π(aromatic) bonds. In the ν(N–H) region, we observe two absorptions centered at 3472 and 3426 cm^{-1} (Fig. 5, trace e) that we assign to ν(N–H) of slightly perturbed IN involved in ≡Si–O–H···π(aromatic) interactions and to N–H···O(H)–Si≡ bonds, respectively. Indeed, in CCl_4 solution, ν(N–H) for monomeric IN and N–H···π(aromatic) are observed at 3489 and 3424 cm^{-1} [26a], respectively, while RIDIR spectra of IN-water clusters show a N–H···OH_2 stretching band at 3436 cm^{-1} [29].

It is worth noting that on the surface of $Ru(II)/SiO_2$ there are almost exclusively silanols in hydrogen bonding to the oxygen atoms of the sulfonate groups (Fig. 4a) and therefore the N–H···O(H)–Si≡ interactions should persist, as they do not need the presence of isolated silanols to occur (Scheme 1).

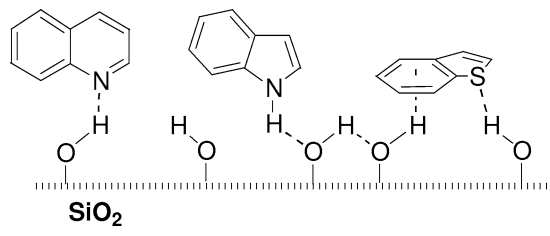

Scheme 1.

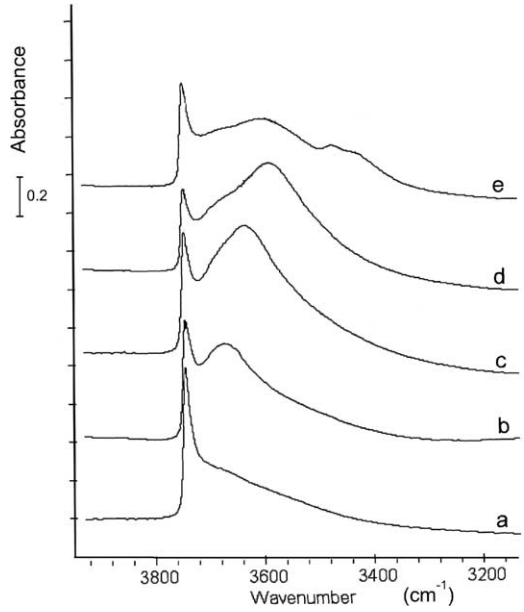

Fig. 5. FTIR transmission spectra in the ν(O–H) region of heterocyclic compounds adsorbed on silica pellets: (a) pure SiO_2; (b) Q/SiO_2; (c) BT/SiO_2; (d) $MeIN/SiO_2$; (e) IN/SiO_2.

3.3. Hydrogenation of S- and N-heterocycles

3.3.1. Benzo[b]thiophene and dibenzo[b, d]thiophene

Selected data relative to the hydrogenation of BT are reported in Table 3. Under the experimental conditions employed in this work, $Ru(0)/SiO_2$ did not catalyze the hydrogenation of BT to any extent (entry 1). In contrast, the Ru(II) single-site catalyst $Ru(II)/SiO_2$ was very active, converting 2000 equivalents of BT selectively to 2,3-dihydrobenzo[*b*]thiophene (DHBT) in 1 h (entry 2). A significantly lower turnover frequency (TOF, expressed as mol of product (mol of cat $\times$ *h*)$^{-1}$) was observed with the homogeneous precursor Ru(II)-triphos in CH_2Cl_2, where the catalytically active Ru species is analogous to that formed in the heterogeneous reaction assisted by $Ru(II)/SiO_2$ (entry 4) [7,15a]. To observe homogeneous activity comparable to that in heterogeneous phase, a polar solvent was used to promote the heterolytic splitting of H_2 at ruthenium, and therefore the reaction involved a different catalyst, a Ru(II) monohydride (entry 5) [7,15a]. However, this catalyst underwent appreciable deactivation in THF and gave a TOF of 760 when a second amount of substrate was injected into the reactor (entry 6), while the heterogeneous catalyst $Ru(II)/SiO_2$ was recycled three times with no significant decay in activity (the TOF was 1960 in the third run). The TOF with $Ru(II)/SiO_2$ did not practically change even when a new feed containing 2000 equiv of BT in 2 ml of *n*-octane was injected into the reactor after 1 h reaction, which means that DHBT does not compete with BT for coordination to ruthenium(II) (entry 3).

As previously reported [15a,b], the deactivation of the homogeneous catalyst in THF involves the conversion of the precursor to the known Ru(II) μ-hydroxo complex $[Ru(\mu\text{-}OH)_3(triphos)]_2(SO_3CF_3)$ that was actually isolated after catalysis. The formation of this catalytically inactive binuclear complex is promoted by bases (e.g., amines) in the reaction mixture that may generate OH^- groups by reaction with adventitious water in the solvent [15a,b]. Therefore, it was not surprising to find that the worst catalyst for the regioselective hydrogenation of BT to DHBT was the aqueous-biphase precursor Ru(II)-sulphos in water–*n*-octane (TOF 30) (entry 7) due to the massive presence of water.

Unlike BT, DBT was not hydrogenated by any of the catalysts investigated irrespective of the metal oxidation state or the phase system.

3.3.2. Quinoline

The heterogeneous catalyst $Ru(0)/SiO_2$ catalyzes the hydrogenation of both the heterocyclic and carbocyclic rings of Q

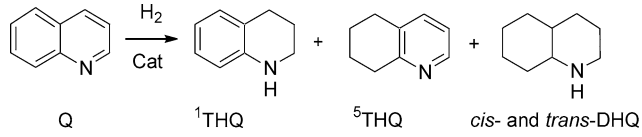

(1)

(see Table 4). For a substrate-to-catalyst ratio of 100, 1,2,3,4-tetrahydroquinoline (^{1}THQ) and 5,6,7,8-tetrahydro-

Table 3
Hydrogenation of BT with ruthenium(0) and ruthenium(II) catalysts in different phase-variation systems[a]

Entry	Catalyst	Phase system (solvent(s))	BT/Ru ratio	DHBT, TOF[b]
1	$Ru(0)/SiO_2$	Heterogeneous (*n*-octane)	100	0
2	$Ru(II)/SiO_2$	Heterogeneous (*n*-octane)	2000	2000
3[c]	$Ru(II)/SiO_2$	Heterogeneous (*n*-octane)	2000	1997
4[d]	Ru(II)-triphos	Homogeneous (CH_2Cl_2)	2000	1340
5[d]	Ru(II)-triphos	Homogeneous (THF)	2000	1990
6[c,d]	Ru(II)-triphos	Homogeneous (THF)	2000	760
7	Ru(II)-sulphos	Biphasic (H_2O/*n*-octane, 1 : 1, v : v)	100	30

[a] Experimental conditions: Ru, 0.022 mmol; H_2 pressure, 30 bar; solvent, 30 ml; temperature, 100 °C; time, 1 h; stirring rate, 1500 rpm.

[b] Mol of product (mol of cat $\times$ h)$^{-1}$; average values over at least three runs.

[c] 2000 equiv of BT was added to the final reaction mixture of entry 2.

[d] Stirring rate 750 rpm.

Table 4
Hydrogenation of Q with ruthenium(0) and ruthenium(II) catalysts in different phase-variation systems[a]

Entry	Catalyst	Phase system (solvent(s))	Products, TOF[b]		
			^{1}THQ	^{5}THQ	*cis*/*trans*-DHQ
1	$Ru(0)/SiO_2$	Heterogeneous (*n*-octane)	49	34	16/1
2[c]	$Ru(0)/SiO_2$	Heterogeneous (*n*-octane)	185	20	4/ < 1
3	$Ru(II)/SiO_2$	Heterogeneous (*n*-octane)	37		
4[d]	$Ru(II)/SiO_2$	heterogeneous (*n*-octane)	16	< 1	
5[e]	Ru(II)-triphos	homogeneous (CH_2Cl_2)	24		
6[d,e]	Ru(II)-triphos	Homogeneous (CH_2Cl_2)	12		
7[e]	Ru(II)-triphos	Homogeneous (THF)	35		
8[d,e]	Ru(II)-triphos	Homogeneous (THF)	11	1	
9	Ru(II)-sulphos	Biphasic (H_2O/*n*-octane, 1 : 1, v : v)	7		

[a] Experimental conditions: Ru, 0.022 mmol; substrate to catalyst ratio, 100; solvent, 30 ml; H_2 pressure, 30 bar; temperature, 100 °C; time, 1 h; stirring rate, 1500 rpm.
[b] Mol of product (mol of cat × h)$^{-1}$; average values over at least three runs.
[c] Substrate to catalyst ratio, 500.
[d] Time, 5 h.
[e] Stirring rate, 750 rpm.

quinoline (^{5}THQ) were obtained in comparable amounts, while *cis*-decahydroquinoline (DHQ) largely prevailed over *trans*-DHQ (entry 1) [2,7b]. Increasing the initial concentration of Q to 500 equivalents resulted in a surprising increase in regioselectivity as ^{1}THQ became the largely prevalent product with a TOF of 185 vs 20 of ^{5}THQ (entry 2), while the production of DHQ isomers was very low.

Complete regioselectivity in ^{1}THQ was obtained with the Ru(II) single-site catalyst (entry 3) that, although intrinsically less active than supported Ru(0), continued to exclusively hydrogenate the heterocyclic ring for 5 h (entry 4).

Selectivity of the same type as that of the heterogeneous single-site catalyst $Ru(II)/SiO_2$ was obtained also in homogeneous phase with Ru(II)-triphos in either CH_2Cl_2 (entry 5) or THF (entry 7). In contrast, the catalytic performance was improved upon immobilization, especially as regards the catalyst activity (entries 3 and 5) and the catalyst durability (entries 3 and 4 vs 7 and 8). Again, the formation of the catalytically inactive μ-hydroxo compound led to small activity of the aqueous-biphase catalyst (entry 9) [15a,b].

3.3.3. Acridine

As with Q, $Ru(II)/SiO_2$ gave exclusive hydrogenation of the heterocyclic ring of AC

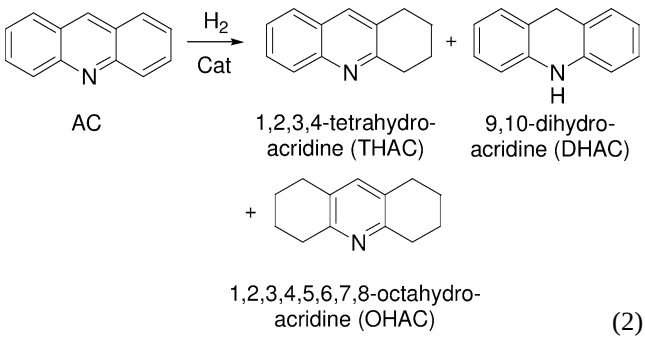

(2)

with the formation of 9,10-dihydroacridine (DHAC) at a fairly good rate (entry 2, Table 5), while the Ru(0) catalyst, although slightly more active on the whole, was less selective leading to reduction of both internal and external rings (entry 1).

The homogeneous catalyst Ru(II)-triphos in either CH_2Cl_2 or THF (entries 4 and 6) was as selective as the immobilized one (entry 2). Again, the least stable catalyst was generated by Ru(II)-triphos in THF, as shown by the decrease in TOF after 5 h.

Table 5
Hydrogenation of AC with ruthenium(0) and ruthenium(II) catalysts in different phase-variation systems[a]

Entry	Catalyst	Phase system (solvent(s))	Products, TOF[b]		
			THAC	DHAC	OHAC
1	$Ru(0)/SiO_2$	Heterogeneous (*n*-octane)	24	26	6
2	$Ru(II)/SiO_2$	Heterogeneous (*n*-octane)		50	
3[c]	$Ru(II)/SiO_2$	Heterogeneous (*n*-octane)		18	< 1
4[d]	Ru(II)-triphos	Homogeneous (CH_2Cl_2)		42	
5[c,d]	Ru(II)-triphos	Homogeneous (CH_2Cl_2)		16	
6[d]	Ru(II)-triphos	Homogeneous (THF)		50	< 1
7[c,d]	Ru(II)-triphos	Homogeneous (THF)		13	

[a] Experimental conditions: Ru, 0.022 mmol; substrate to catalyst ratio, 100; solvent, 30 ml; H_2 pressure, 30 bar; temperature, 100 °C; time, 1 h; stirring rate, 1500 rpm.
[b] Mol of product (mol of cat × h)$^{-1}$; average values over at least three runs.
[c] Time, 5 h.
[d] Stirring rate, 750 rpm.

Table 6
Hydrogenation of IN with ruthenium(0) and ruthenium(II) catalysts in different phase-variation systems[a]

Entry	Catalyst	Phase system (solvent(s))	Products, TOF[b]		
			INE	THIN	OHIN
1	$Ru(0)/SiO_2$	Heterogeneous (*n*-octane)	9	9	47
2	$Ru(II)/SiO_2$	Heterogeneous (*n*-octane)	14		
3[c,d]	Ru(II)-triphos	Homogeneous (THF or CH_2Cl_2)	< 1		
4[c,d,e]	Ru(II)-triphos	Homogeneous (THF)	17		

[a] Experimental conditions: Ru, 0.022 mmol; substrate to catalyst ratio, 100; solvent, 30 ml; H_2 pressure, 30 bar; temperature, 100 °C; time, 1 h; stirring rate, 1500 rpm.
[b] Mol of product (mol of cat × h)$^{-1}$; average values over at least three runs.
[c] See Ref. [15d].
[d] Stirring rate, 750 rpm.
[e] 40 N of CF_3SO_3H.

3.3.4. Indole

Indoline (INE), 4,5,6,7-tetrahydroindole (THIN), and octahydro-1*H*-indole (OHIN) were obtained by hydrogenation of IN

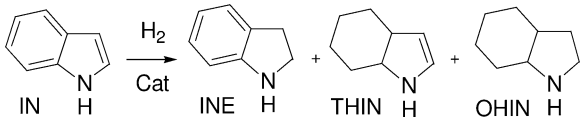

(3)

with $Ru(0)/SiO_2$ (entry 1, Table 6). The immobilized Ru(II) catalyst was less efficient but more selective than the Ru(0) one as only INE was produced with a TOF of 14 (entry 2). For this substrate, almost no hydrogenation was observed using the homogeneous catalyst in either CH_2Cl_2 or THF (entry 3) even for reaction times as long as 5 h [15d].

3.4. Competitive hydrogenation reactions

The first mixture of substrates under examination was constituted by Q and IN in a 1 : 1 ratio. The hydrogenation results obtained with $Ru(0)/SiO_2$ and $Ru(II)/SiO_2$ are reported in Table 7. The co-presence of IN and Q had a surprising effect on both activity and selectivity of the Ru(0) catalyst: Q apparently inhibits the hydrogenation of IN, which was produced in only 10% yield (entry 1) vs 65% with no added competitor (Table 6, entry 1). Moreover, only INE was produced. In turn, the presence of IN decreased the overall hydrogenation of Q and also changed the regioselectivity (see Table 4, entry 1): ^{1}THQ was the largely predominant product (78% vs 7% of ^{5}THQ), while the formation of the two DHQs was suppressed.

The contemporaneous presence of Q and IN in the reaction mixture did not practically affect their hydrogenation to ^{1}THQ and INE, respectively, by the Ru(II) single-site catalyst (entry 2); in particular, the conversion of IN was identical to that obtained in the absence of Q, while a slight decrease was observed for Q.

Table 7
Hydrogenation of Q/IN with silica-supported ruthenium(0) and ruthenium(II) catalysts[a]

Entry	Catalyst	Products, TOF[b]					
		^{1}THQ	^{5}THQ	*cis*-DHQ	INE	THIN	OHIN
1	$Ru(0)/SiO_2$	78	7		10		
	[c]	(49)	(34)	(16)			
	[d]				(9)	(9)	(47)
2	$Ru(II)/SiO_2$	30		< 1	14		
	[c]	(37)					
	[d]				(14)		

[a] Experimental conditions: Ru, 0.022 mmol; Q/IN/Ru ratio, 100 : 100 : 1; *n*-octane, 30 ml; H_2 pressure, 30 bar; temperature, 100 °C; time, 1 h; stirring rate, 1500 rpm.
[b] Mol of product (mol of cat × h)$^{-1}$; average values over at least three runs.
[c] In the absence of IN; see Table 4.
[d] In the absence of Q; see Table 6.

It is well known that the strong tendency of nitrogen compounds to adsorb over heterogeneous catalysts may inhibit other hydrotreating reactions [1,2]. To see whether this effect occurs also for the present catalysts, reactions with BT/Q mixtures were carried out. The results obtained are reported in Table 8.

The presence of BT in the same concentration as Q significantly affected the hydrogenation of the *N*-heterocycle with $Ru(0)/SiO_2$ (entry 1): no formation of ^{5}THQ was observed and the overall conversion of Q was lower than that obtained in the absence of BT (see Table 4, entry 1). Doubling the relative concentration of BT resulted in a further decrease of Q conversion (from 56 to 41%) (entry 2). Almost no hydrogenation of BT occurred as found in the reactions without Q (Table 3, entry 1).

A significant decrease in the TOF relative to ^{1}THQ production was observed in the 1-h reaction catalyzed by $Ru(II)/SiO_2$ (entry 4; see also Table 4, entry 3); however,

Table 8
Hydrogenation of BT/Q with silica-supported ruthenium(0) and ruthenium(II) catalysts[a]

Entry	Catalyst	BT/Q/Ru ratio	Products, TOF[b]		
			^{1}THQ	^{5}THQ	DHBT
1	$Ru(0)/SiO_2$	100 : 100 : 1	56		< 1
2	$Ru(0)/SiO_2$	200 : 100 : 1	41		1
3[c]	$Ru(0)/SiO_2$	100 : 100 : 1	36		2
4	$Ru(II)/SiO_2$	100 : 100 : 1	22		> 99
5[d]	$Ru(II)/SiO_2$	100 : 100 : 1	15		20

[a] Experimental conditions: Ru, 0.022 mmol; *n*-octane, 30 ml; H_2 pressure, 30 bar; temperature, 100 °C; time, 1 h; stirring rate, 1500 rpm.
[b] Mol of product (mol of cat × h)$^{-1}$; average values over at least three runs.
[c] Addition followed by hydrogenation of Q was carried out after the catalyst was reacted with BT and H_2 for 1 h at 100 °C.
[d] Time, 5 h.

Table 9
Hydrogenation of aromatics with silica-supported ruthenium(0) nanoparticles[a]

Entry	Catalyst	Substrate	Products, TOF[b]
1	$Ru^{(0)}/SiO_2$	TO	MeCy 360
2	$Ru^{(0)}/SiO_2$	AN	THAN 14; DHAN < 1; OHAN 1

[a] Experimental conditions: Ru, 0.022 mmol; substrate to catalyst ratio, 500 (entry 1) and 100 (entry 2); *n*-octane, 30 ml; H_2 pressure, 30 bar; temperature, 100 °C; time, 1 h; stirring rate, 1500 rpm.

[b] Mol of product (mol of cat × h)$^{-1}$; average values over at least three runs.

when all BT was consumed, the hydrogenation of Q proceeded as fast as with Q alone (entry 5, see also Table 4, entry 4).

3.5. Hydrogenation of arenes

Neither toluene (TO) nor anthracene (AN) was hydrogenated by the Ru(II) single-site catalyst. In contrast, $Ru(0)/SiO_2$ was rather active for the conversion of TO to methylcyclohexane (MeCy)

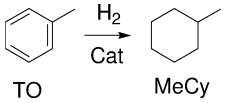

(4)

(see Table 9) and, to a smaller extent, of AN to 1,2,3,4-tetrahydroanthracene (THAN)

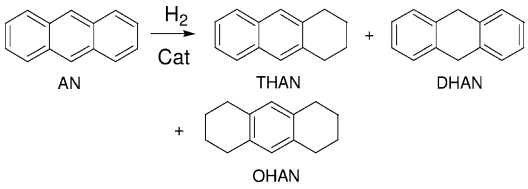

(5)

(see Table 9). Also, only traces of the other two possible hydrogenation products of AN, 9,10-dihydro-anthracene (DHAN) and 1,2,3,4,5,6,7,8-octahydro-anthracene (OHAN), were obtained (entry 2).

4. Discussion

4.1. Hydrogenation of S- and N-heterocycles

Under the experimental conditions employed in this work, the polyaromatic heterocycles shown in Chart 2 are hydrogenated by both $Ru(II)/SiO_2$ and $Ru(0)/SiO_2$ to cyclic thioethers or amines with no apparent hydrogenolysis. These hydrogenation steps are of crucial importance for the HDS and HDN of *S*- and *N*-heterocycles [1–8].

The transformations undergone by the present Ru(II) catalysts upon hydrogenation with 30-bar H_2 in different phase variation systems have been studied previously (Scheme 2) [13b,15,30].

It has been demonstrated that $Ru(II)/SiO_2$ is converted to silica-grafted $[(sulphos)Ru(H)_2L]^+$ complex, where L is either intact H_2, MeCN, or a molecule derived from the hydrogenation of MeCN [13b]. In any case, L is a weakly bonded group that can be easily displaced by the substrate to reduce (Scheme 2a). The recovery of the $[(sulphos)Ru(H)_2L]^+$ moieties at the end of the catalytic hydrogenation reactions is achieved by treatment of the heterogeneous catalyst with MeOH that disrupts the hydrogen-bond interactions between the metal complex and the support surface.

The homogeneous precursor Ru(II)-triphos reacts with H_2 in THF to give a monohydride Ru(II)–H species via H_2 heterolytic splitting [13b,15,30], whereas in nonbasic solvents such as CH_2Cl_2, no heterolytic splitting occurs and $[(triphos)Ru(H)_2L]^{2+}$ species (L = $NHEt_2$, NH_3, MeCN) are formed (Scheme 2b). In conclusion, $Ru(II)/SiO_2$ works in hydrogenation reactions performed in *n*-octane as a Ru(IV) dihydride, while Ru(II)-triphos can behave as either a Ru(IV) dihydride or a Ru(II) monohydride, depending on the solvent.

For all reactions investigated, HPNMR spectra were recorded in C_6D_6 slurries containing $Ru(II)/SiO_2$ and a 20-fold excess of substrate, applying the same experimental conditions as in the batch catalytic runs (30 bar H_2, 100 °C). In no case was Ru-sulphos leaching observed during catalysis (i.e., no $^{31}P\{^1H\}$ NMR signal was detected), while ^1H NMR spectroscopy showed the formation of hydrogenation products. The lack of any $^{31}P\{^1H\}$ NMR signal during and after the catalysis ruled out the occurrence of homogeneous reactions involving ruthenium catalysts kept close to the silica surface only by electrostatic interaction with anchored triflate counteranions. Were this the case, as previously reported for optically active cationic diphosphine–rhodium catalysts immobilized to silica via hydrogen bonding [13a,14], $^{31}P\{^1H\}$ NMR signals would have been observed with the typical band broadening due to restricted mobility of the cations on the silica surface.

4.1.1. Benzo[b]thiophene

The mechanism of hydrogenation/hydrogenolysis of BT by homogeneous ruthenium catalysts has been the subject of several studies [4–7]. It is agreed that the regioselective reduction of the heterocyclic ring involves the η^2-C_2–C_3 coordination of BT to high-valent ruthenium centers (either Ru(II) or Ru(IV)), followed by *cis*-hydride transfer. This mechanism is probably operative also for $Ru(II)/SiO_2$ (Scheme 3a) which, like Ru(II)-triphos, is not active for the hydrogenation of DBT [13b,15a,30,31]. Generally, in fact, there is no significant change in reaction mechanism when a metal site is transferred from solution to a solid surface [9].

The failure in the hydrogenation of BT and DBT by $Ru(0)/SiO_2$ cannot be related to low propensity to adsorb sulfur compounds over supported Ru(0); rather we think that the adsorption of BT onto the surface of $Ru(0)/SiO_2$ most likely in the η^1-*S* mode, does occur under the experimental conditions investigated in this work (Scheme 3b).

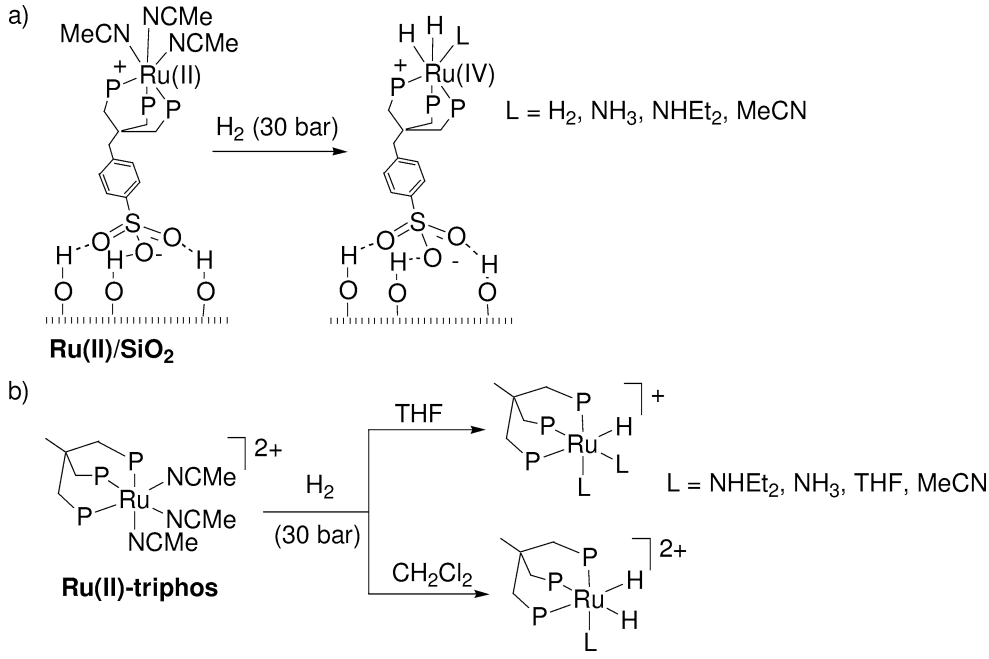

Scheme 2.

Heterogeneous ruthenium catalysts are quite efficient for the deep HDS of thiophenes, in fact, albeit at 400–600 °C and H_2 pressures higher than 100 bar [1a,b], with mechanisms that have been proposed to involve η^1-*S* coordination of the thiophene prior to C–S bond scission and hydrogenolysis [1,2]. Moreover, Ru(0) fragments such as [Ru(PP_3)] were reported to bind thiophenes in η^1-*S* fashion (Scheme 3c), forming stable adducts that do not undergo hydrogenation of the bonded thiophene [$PP_3 = P(CH_2CH_2PPh_2)_3$] [32]. It is very likely that Ru(0)/SiO_2 behaves like [Ru(PP_3)]: BT is selectively adsorbed in the η^1-*S* mode over the ruthenium atoms (Scheme 3b), but it is neither hydrogenated, because of the unfavorable orientation, nor C–S inserted, due to the mild reaction conditions.

4.1.2. Quinoline

The hydrogenation of Q by soluble metal complexes has been investigated by several authors [2,7b,8,33]. It is agreed that *N*-bonding of Q to the metal is necessary for selective hydrogenation to ^{1}THQ. In some cases, an η^1-*N* to η^2-*C*,*N* shift prior to hydride migration has been postulated. A few examples of η^6-C_6 coordination of Q have been reported [34]. In no case, however, was the catalytic hydrogenation of either ring observed [34]. A direct hydride transfer to the 4-position of η^1-*N* Q, as occurs on real Co-Mo/γ-Al_2O_3 catalysts [1,2], was demonstrated for the clusters $H_2Os_3(CO)_{10}$ and $Os_3(CO)_{12}$, leading to ^{5}THQ [35].

Recent studies from this laboratory suggest that the hydrogenation of Q to ^{1}THQ with Ru(II)-triphos in either CH_2Cl_2 or THF/protic acid proceeds via a mechanism involving η^1-*N* coordination followed by C=N hydrogenation [33]. It is very likely that Ru(II)/SiO_2 follows the same mechanism to hydrogenate Q to ^{1}THQ. In turn, ^{1}THQ may be produced by Ru(0)/SiO_2 via direct 1,4-hydrogen transfer, while ^{5}THQ should be produced by hydrogenation of

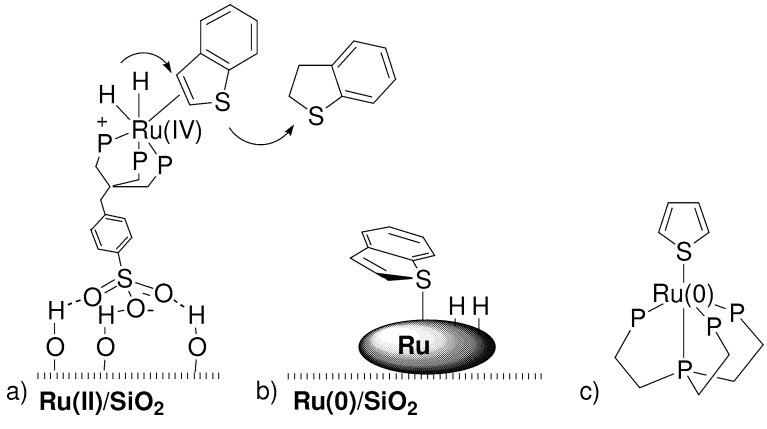

Scheme 3.

adsorbed Q in the η^6-C_6 mode [2,7b]. Indeed, increasing the concentration of Q was found to decrease the ^{5}THQ production, which is consistent with the η^1-N adsorption mode prevailing over the η^6-C_6 one [34].

4.1.3. Acridine

Scarce information on the mechanism for the selective hydrogenation of the central ring of AC by single-site catalysts is available in the relevant literature [36,37]. It is generally believed that AC is reduced to THAC via a mechanism involving direct 9,10-hydrogen transfer [35]. Both η^1-N and carbocyclic η^6-C_6 adsorption modes are possible on Ru(0) nanoparticles and therefore different mechanisms may operate, which accounts for the variety of products obtained.

4.1.4. Indole

It has been recently found in this laboratory that the hydrogenation of IN to INE by homogeneous ruthenium(II) (entry 4, Table 6) and rhodium(III) catalysts can be effectively accomplished only in the presence of a protic acid [15d].

The protic acid is required to generate an equilibrium concentration of the 3H-indolium cation that contains a localized, hence reducible, C=N bond (Scheme 4). On the other hand, the use of protic acids to promote the hydrogenation of IN is a common procedure in heterogeneous catalysis, for example with nickel Raney or copper chromate catalysts [38].

As for the hydrogenation of IN with Ru(II)/SiO_2, we disregard the formation of 3H-indolium cation, as it needs strong acids to occur: even trifluoroacetic acid and *p*-toluenesulfonic acid give incomplete protonation of IN, leading to an equilibrium concentration of 3H-indolium [39]. Therefore, neither isolated silanols of silica (p$K_a > 9$) nor hydrogen-bonded silanols (pK_a 5–7) should be able to protonate IN. We suggest that the hydrogen interactions between the N–H proton of IN and the oxygen atoms of the silanols groups (either isolated or, much more likely, engaged in hydrogen bonding to the sulfonate groups) may activate the heterocyclic ring to expose a more localized, hence reducible, C_2–C_3 bond to ruthenium. A pictorial view of the whole bonding framework that would allow the hydrogenation of IN to INE by immobilized Ru(II) single site is shown in Scheme 5.

Strong support for the positive influence of N–H···O(H)–Si≡ bonds on IN hydrogenation by Ru(II)/SiO_2 was provided by the use of MeIN in the place of IN. The protection

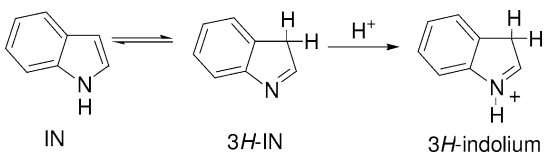

Scheme 4.

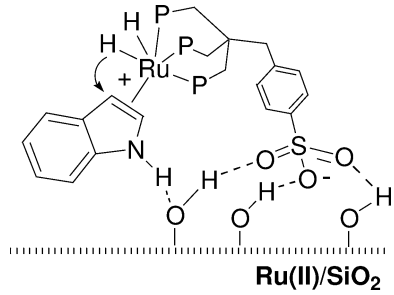

Scheme 5.

of the nitrogen atom with a methyl group did not allow for substrate hydrogenation in fact.

Silica surface-mediated reactions are a relatively new synthetic protocol leading to interesting results in terms of both activity and selectivity as well as environmental friendliness [9,40]. The reactions can be conducted by simple mixing of silica, reagent, and substrate in the dry state followed by heating, while the products are generally extracted from the adsorbent with an appropriate solvent. Mediation by silica was found to involve either isolated or associated silanols. Recent examples of silica surface-mediated reactions with a mechanism similar to that shown in Scheme 5 include the oxidation of sulfides and sulfoxides by *tert*-butyl hydroperoxide [40e].

4.2. Competitive hydrogenation reactions

All the hydrogenation reactions described in this paper were performed at relatively high H_2 pressure and a stirring rate that ensured constant conversions over consecutive runs. Nevertheless, the absence of mass transport effects affecting the hydrogenation rate of each substrate cannot be ruled out [41]. Therefore, the competitive experiments reported in Tables 7 and 8 can be interpreted only on a pure qualitative basis.

The grafted molecular complex Ru(II)/SiO_2 hydrogenates an equimolar mixture of Q and IN with conversions and selectivities that do not substantially differ from those observed for the separate substrates (Table 7). This suggests that Q and IN do not compete for coordination to the metal center. In contrast, the hydrogenation of Q by the same catalyst is remarkably slowed down, yet not inhibited, by the presence of BT (Table 8, entry 4).

Competitive adsorption of the substrates on the ruthenium nanoparticles may also account for the hydrogenation of Q/IN and Q/BT mixtures over Ru(0)/SiO_2. Previous studies have shown that Q uses preferentially the nucleophilic nitrogen atom for coordination, while the coordination of IN occurs exclusively in the sterically demanding η^6-C_6 mode [7b]. The adsorption of nitrogen compounds over heterogeneous Ru-based catalysts is generally very efficient [1a,b,4,7,15], yet not all molecules undergo HDN, due to competing effects of the different substrates leading to unfavorable orientations. The change in hydrogenation selectivity of Q (almost exclusive formation of ^{1}THQ) may

just be due to such an effect: the adsorption of Q in the η^1-*N* mode, which is necessary for selective hydrogenation of the nitrogen ring, is not hampered by IN, which, in contrast, competes with Q to occupy the ruthenium sites that are appropriate for η^6-C_6 adsorption. The increased regioselectivity in Q hydrogenation obtained with $Ru(0)/SiO_2$ in the presence of BT may be attributed to favored η^1-*S* adsorption of BT that would crowd the catalyst surface, disfavoring the η^6-C_6 adsorption of Q. The favored adsorption of the "soft" sulfur compound η^1-*S* fashion over the Ru(0) catalyst surface would also account for the inhibiting effect of BT on the hydrogenation of Q. Indeed, when the catalyst was previously treated with BT in hydrogenation conditions and then used for the hydrogenation of Q, the TOF relative to ^{1}THQ production decreased from 56 to 36 (Table 8, entry 3).

4.3. Arenes

The failure of the single-site catalyst $Ru(II)/SiO_2$ in hydrogenating aromatic hydrocarbons reflects the low propensity of sterically congested metal complexes to coordinate arenes as well as the high activation energy barrier needed to overcome their resonance stabilization energy [12t,34e]. Critical to arene hydrogenation by transition metal complexes is η^4-coordination [42], which has never been obtained with triphosruthenium fragments. An iridium(I) complex, namely $[Ir(\eta^4\text{-}C_6H_6)(triphos)]^+$, exists and readily forms cyclohexane upon hydrogenation [43]. However, even this iridium complex was synthesized by acetylene trimerization, and not by direct reaction with benzene [44]. On the other hand, $[RuH_3(PPh_3)_3]^-$ was found to hydrogenate AN to THAN via a $[RuH(PPh_3)_2(\eta^4\text{-AN})]^-$ intermediate [42], which means that electron-rich ruthenium complexes with appropriate steric hindrance can lower the energy barrier to η^4-coordination of arenes, thus allowing their hydrogenation.

The activity of supported Ru(0) particles in hydrogenating arenes is well documented [45,46]. In general, however, the hydrogenation of simple arenes, such as benzene, leads selectively to the cyclic enes even under drastic reaction conditions. The noticeable activity exhibited by $Ru(0)/SiO_2$ (Table 9) is motivating current studies in our laboratory.

5. Conclusions

For the first time, a molecular Ru(II) complex tethered to a rigid inorganic support has been found able to hydrogenate *S*- and *N*-heterocycles efficiently under mild conditions.

Studies of the variation of the hydrotreating activity exhibited by transition metal sulfides as a function of the position of the metal in the periodic table agree is locate ruthenium at the top of the curve for HDS and in a middle position for HDN [1,2]. The results reported in this work confirm this trend and beyond. It has been shown in fact that Ru(II)-based catalysts are much more efficient for the hydrogenation of *S*-heterocycles, here exemplified by BT, than for the hydrogenation of *N*-heterocycles. Moreover, the results obtained allow one to attempt a correlation between ruthenium oxidation state and hydrogenation activity/selectivity. The Ru(II) single-site catalyst is active for both *S*- and *N*-heterocycles, while the Ru(0) catalyst does not hydrogenate the *S*-heterocycles, yet is efficient for the reduction of *N*-heterocycles and simple aromatic hydrocarbons. The Ru(II) catalyst is more efficient for the hydrogenation of *S*-heterocycles than for the hydrogenation of *N*-heterocycles and is also much more selective than the Ru(0) catalyst for the reduction of *N*-heterocycles due to the preferred η^1-*N* coordination.

In this paper, it has been also shown that the surface silanols promote the hydrogenation of indole via N–H···O(H)–Si≡ hydrogen-bonds and can interact with the π-electron density of all substrates. Of course, such effects are not limited to silica or to the substrates investigated in this work since the surface of several real hydrotreating catalysts may contain both S–H and O–H groups. Therefore, detailed knowledge of the possible interactions between surface/substrate/single-metal site might be extremely useful for designing improved hydrotreating catalysts.

Acknowledgments

The authors thank Dr. S. Marengo for porosimetric measurements performed at the Stazione Sperimentale per i Combustibili S. Donato Milanese (Milano, Italy). Contributions from Agenzia 2000 (CNR, Roma) and the CNR–RAS bilateral agreement (CNR, Roma, Italy) are gratefully acknowledged. This research has also been supported by a Marie Curie Individual Fellowship of the European Community program "Heterogenization of Chiral and Achiral Molecular Catalysis" under Contract HPMF-CT-2000-00568.

References

[1] (a) T. Kabe, A. Ishihara, W. Qian, Hydrodesulfurization and Hydrodenitrogenation, Wiley/VCH, Tokyo, 1999;
(b) H. Topsøe, B.S. Clausen, F.E. Massoth, Hydrotreating Catalysis, Springer, Berlin/Heidelberg, 1996;
(c) J. Scherzer, A.J. Gruia, Hydrocracking Science and Technology, Dekker, New York, 1996;
(d) M.L. Occelli, R. Chianelli, Hydrotreating Technology for Pollution Control, Dekker, New York, 1996.

[2] (a) B.C. Wiegand, C.M. Friend, Chem. Rev. 92 (1992) 491;
(b) M.J. Girgis, B.C. Gates, Ind. Eng. Chem. Res. 30 (1991) 2031;
(c) T.C. Ho, Catal. Rev. Sci. Eng. 30 (1988) 117;
(d) R.M. Laine, Catal. Rev. Sci. Eng. 25 (1983) 459;
(e) J.R. Katzer, R. Sivasubramanian, Catal. Rev. Sci. Eng. 20 (1979) 155;
(f) B.C. Gates, J.R. Katzer, G.C.A. Schuit, Chemistry of Catalytic Processes, McGraw–Hill, New York, 1979.

[3] (a) J.V. Lauritsen, S. Helveg, E. Lægsgaard, I. Stensgaard, B.S. Clausen, H. Topsøe, F. Besenbacher, J. Catal. 197 (2001) 1;

(b) A.N. Startsev, Catal. Rev. Sci. Eng. 37 (1995) 353.
[4] (a) R.J. Angelici, Organometallics 20 (2001) 1259;
(b) J. Chen, R.J. Angelici, Coord. Chem. Rev. 206–207 (2000) 63;
(c) R.J. Angelici, in: T. Weber, R. Prins, R.A. van Santen (Eds.), Transition Metal Sulphides—Chemistry and Catalysis, Kluwer Academic, Dordrecht, 1998, p. 89;
(d) R.J. Angelici, Polyhedron 16 (1997) 3073;
(e) R.J. Angelici, Bull. Soc. Chim. Belg. 104 (1995) 265;
(f) R.J. Angelici, in: R.B. King (Ed.), Encyclopedia of Inorganic Chemistry, Vol. 3, Wiley, New York, 1994, p. 1433;
(g) R.J. Angelici, Coord. Chem. Rev. 105 (1990) 61;
(h) R.J. Angelici, Acc. Chem. Res. 21 (1988) 387.
[5] T.B. Rauchfuss, Prog. Inorg. Chem. 39 (1991) 259.
[6] R.A. Sánchez-Delgado, J. Mol. Catal. 86 (1994) 287.
[7] (a) C. Bianchini, A. Meli, in: B. Cornils, W.A. Herrmann (Eds.), Applied Homogeneous Catalysis with Organometallic Compounds, 2nd ed., VCH, Weinheim, Germany, 2002, p. 1099;
(b) C. Bianchini, A. Meli, F. Vizza, Eur. J. Inorg. Chem. (2001) 43;
(c) C. Bianchini, A. Meli, in: T. Weber, R. Prins, R.A. van Santen (Eds.), Transition Metal Sulphides—Chemistry and Catalysis, Kluwer Academic, Dordrecht, 1998, p. 129;
(d) C. Bianchini, A. Meli, Acc. Chem. Res. 31 (1998) 109;
(e) C. Bianchini, A. Meli, in: B. Cornils, W.A. Herrmann (Eds.), Aqueous-Phase Organometallic Catalysis—Concepts and Applications, VCH, Weinheim, Germany, 1998, p. 477;
(f) C. Bianchini, A. Meli, in: B. Cornils, W.A. Herrmann (Eds.), Applied Homogeneous Catalysis with Organometallic Compounds, Vol. 2, VCH, Weinheim, Germany, 1996, p. 969;
(g) C. Bianchini, A. Meli, J. Chem. Soc. Dalton Trans. (1996) 801.
[8] K.J. Weller, P.A. Fox, S.D. Gray, D.E. Wigley, Polyhedron 16 (1997) 3139.
[9] (a) F.T. Hartley, Supported Metal Complexes, Reidel, Dordrecht, 1985;
(b) B.E. Hanson, in: R.B. King (Ed.), Encyclopedia of Inorganic Chemistry, Vol. 7, Wiley, New York, 1994, p. 4056;
(c) P. Panster, S. Wieland, in: B. Cornils, W.A. Herrmann (Eds.), Applied Homogeneous Catalysis with Organometallic Compounds, VCH, Weinheim, Germany, 1996, p. 605;
(d) B. Cornils, W.A. Herrmann, in: B. Cornils, W.A. Herrmann (Eds.), Applied Homogeneous Catalysis with Organometallic Compounds, VCH, Weinheim, Germany, 1996, p. 575;
(e) E. Lindner, T. Schneller, F. Auer, H.A. Mayer, Angew. Chem., Int. Ed. Engl. 38 (1999) 2155;
(f) C. Bianchini, P. Barbaro, Topics Catal. 19 (2002) 17.
[10] (a) C. Bianchini, M. Frediani, F. Vizza, J. Chem. Soc. Chem. Commun. (2001) 479;
(b) C. Bianchini, M. Frediani, G. Mantovani, F. Vizza, Organometallics 20 (2001) 2660.
[11] E.F. Vansant, P. Van DerVoort, K.C. Vrancken, in: B. Delmon, J.T. Yates (Eds.), in: Studies in Surface Science and Catalysis, Vol. 93, Elsevier, Amsterdam, 1995.
[12] (a) J.-F. Carpentier, F. Agbossou, A. Mortreux, Tetrahedron 6 (1995) 39;
(b) M.G. Petrucci, A.K. Kakkar, J. Chem. Soc. Chem. Commun. (1995) 1577;
(c) J.-A.M. Andersen, A.W.S. Currie, J. Chem. Soc. Chem. Commun. (1996) 1543;
(d) K.D. Behringer, J. Blümel, J. Chem. Soc. Chem. Commun. (1996) 654;
(e) M. Zhou, J.M. Laux, K.D. Edwards, J.C. Hemminger, B. Hong, J. Chem. Soc. Chem. Commun. (1997) 1977;
(f) Y.V. Rao Subba, D.E. DeVos, T. Bein, P.A. Jacobs, J. Chem. Soc. Chem. Commun. 355 (1997);
(g) R. Neumann, T.-J. Wang, J. Chem. Soc. Chem. Commun. (1997) 1915;
(h) A.W. Kaplan, R.G. Bergman, Organometallics 17 (1998) 5072;
(i) R. Rao Ramachandra, B.M. Weckhuysen, R.A. Schoonheydt, J. Chem. Soc. Chem. Commun. (1999) 445;
(j) J. Büchele, H.A. Mayer, J. Chem. Soc. Chem. Commun. (1999) 2165;
(k) S.-G. Shyu, S.-W. Cheng, D.-L. Tzou, J. Chem. Soc. Chem. Commun. (1999) 2337;
(l) B.F.G. Johnson, S.A. Raynor, D.S. Shephard, T. Mashmeyer, J.T. Meurig, S. Gopinthar, S. Bromey, R. Oldroyd, L. Gladden, M.D. Mantle, J. Chem. Soc. Chem. Commun. (1999) 1167;
(m) H.H. Wagner, H. Hausmann, W.F. Holderich, J. Catal. 203 (2001) 150;
(n) H. Gao, R.J. Angelici, J. Am. Chem. Soc. 119 (1997) 6937;
(o) H. Gao, R.J. Angelici, New J. Chem. 23 (1999) 633;
(p) H. Yang, H. Gao, R.J. Angelici, Organometallics 18 (1999) 2285;
(q) H. Gao, R.J. Angelici, Organometallics 18 (1999) 989;
(r) H. Gao, R.J. Angelici, J. Mol. Catal. A Chem. 145 (1999) 83;
(s) H. Gao, R.J. Angelici, J. Mol. Catal. A Chem. 149 (1999) 63;
(t) H. Yang, H. Gao, R.J. Angelici, Organometallics 19 (2000) 622.
[13] (a) C. Bianchini, P. Barbaro, V. Dal Santo, R. Gobetto, A. Meli, W. Oberhauser, R. Psaro, F. Vizza, Adv. Synth. Catal. 343 (2001) 41;
(b) C. Bianchini, V. Dal Santo, A. Meli, W. Oberhauser, R. Psaro, F. Vizza, Organometallics 19 (2000) 2433;
(c) C. Bianchini, D.G. Burnaby, J. Evans, P. Frediani, A. Meli, W. Oberhauser, R. Psaro, L. Sordelli, F. Vizza, J. Am. Chem. Soc. 121 (1999) 5961.
[14] F.M. De Rege, D.K. Morita, K.C. Ott, W. Tumas, R.D. Broene, J. Chem. Soc. Chem. Commun. 1797 (2000).
[15] (a) C. Bianchini, A. Meli, S. Moneti, W. Oberhauser, F. Vizza, V. Herrera, A. Fuentes, R.A. Sánchez-Delgado, J. Am. Chem. Soc. 121 (1999) 7071;
(b) C. Bianchini, A. Meli, S. Moneti, F. Vizza, Organometallics 17 (1998) 2636;
(c) C. Bianchini, D. Masi, A. Meli, M. Peruzzini, F. Vizza, F. Zanobini, Organometallics 17 (1998) 2495;
(d) P. Barbaro, C. Bianchini, A. Meli, M. Moreno, F. Vizza, Organometallics 31 (2002) 1430.
[16] E.P. Barrett, L.G. Joyner, P.P. Halenda, J. Am. Chem. Soc. 73 (1951) 373.
[17] S. Brunauer, P.H. Emmett, E. Teller, J. Am. Chem. Soc. 60 (1938) 309.
[18] L.F. Rhodes, C. Sorato, L.M. Venanzi, F. Bachechi, Inorg. Chem. 27 (1988) 604.
[19] C. Roveda, E. Cariati, E. Lucenti, D. Roberto, J. Organomet. Chem. 580 (1999) 117.
[20] C. Bianchini, A. Meli, A. Traversi, Italian Patent FI A000025, CNR, 1997.
[21] R. Psaro, R. Ugo, G.M. Zanderighi, B. Besson, A.K. Smith, J.K. Basset, J. Organomet. Chem. 213 (1981) 215.
[22] N. Binsted, PAXAS programme for the analysis of X-ray absorption spectra, University of Southampton, Southampton, 1988.
[23] B. Lengeler, E.P. Eisenberger, Phys. Rev. B 21 (1980) 4507.
[24] (a) S.J. Gurman, N. Binsted, J. Ross, J. Phys. Chem. 17 (1984) 143;
(b) S.J. Gurman, N. Binsted, J. Ross, J. Phys. Chem. 19 (1986) 1845.
[25] (a) F.A.R. Kaul, G.T. Puchta, H. Schneider, F. Bielert, D. Mihalios, W.A. Herrmann, Organometallics 21 (2002) 74;
(b) H.H. Wagner, H. Hausmann, W.F. Hölderich, J. Catal. 203 (2001) 150.
[26] (a) V. Stefov, Lj. Pejov, B. Šoptrajanov, J. Mol. Struct. 555 (2000) 363;
(b) M.A. Munoz, O. Sama, M.L. Galan, P. Guardado, C. Carmona, M.J. Balon, Phys. Chem. B 103 (41) (1999) 8794;
(c) C.H. Rochester, D.A. Trebilco, Chem. Ind. (1978) 248;
(d) W. Pohle, J. Chem. Soc. Faraday Trans. 1 78 (1982) 2101;
(e) T. Steiner, Angew. Chem. Int. Ed. 41 (2002) 49.
[27] W.A. Remers, in: W.J. Houlihan (Ed.), Heterocyclic Compounds, Interscience, New York, 1972.
[28] The low solubility of the complex did not allow the impregnation on silica wafers for FTIR studies; analogously, DRIFT spectroscopy in flow conditions on powder samples could not be used, as our apparatus

does not allow one to introduce liquid solutions or gases of high boiling substrates such as those investigated in this work.
[29] J.R. Carney, T.S. Zwier, J. Phys. Chem. A 103 (1999) 9943.
[30] V.I. Bakhmutov, E.V. Bakhmutova, N.V. Belkova, C. Bianchini, L.M. Epstein, D. Masi, M. Peruzzini, E.S. Shubina, E. Vorontsov, F. Zanobini, Can. J. Chem. 79 (2001) 479.
[31] R. Poli, M. Peruzzini (Eds.), Recent Advances in Hydride Chemistry, Elsevier, Amsterdam, 2001.
[32] (a) R. Osman, D.I. Pattison, R.N. Perutz, C. Bianchini, J.A. Casares, M. Peruzzini, J. Am. Chem. Soc. 119 (1997) 8459;
(b) C. Bianchini, J.A. Casares, R. Osman, D.I. Pattison, M. Peruzzini, R.N. Perutz, F. Zanobini, J. Organometallics 16 (1997) 4611.
[33] C. Bianchini, P. Barbaro, M. Macchi, A. Meli, F. Vizza, Helv. Chim. Acta 84 (2001) 2895.
[34] (a) E. Baralt, S.J. Smith, J. Hurwitz, I.T. Horváth, R.H. Fish, J. Am. Chem. Soc. 114 (1992) 5187;
(b) R.H. Fish, H.-S. Kim, R.H. Fong, Organometallics 10 (1991) 770;
(c) R.H. Fish, R.H. Fong, A. Than, E. Baralt, Organometallics 10 (1991) 1209;
(d) R.H. Fish, E. Baralt, H.-S. Kim, Organometallics 10 (1991) 1965;
(e) R.H. Fish, J.N. Michaels, R.S. Moore, H. Heinemann, J. Catal. 123 (1990) 74;
(f) R.H. Fish, H.-S. Kim, R.H. Fong, Organometallics 8 (1989) 1375.
[35] R.M. Laine, New J. Chem. 11 (1987) 543.
[36] (a) R.H. Fish, J.L. Tan, A. Thormodsen, Organometallics 4 (1985) 1743;
(b) R.H. Fish, J.L. Tan, A. Thormodsen, J. Org. Chem. 49 (1984) 4500.
[37] M. Rosales, J. Navarro, L. Sanchez, A. Gonzales, Y. Alvarado, R. Rubio, C. De la Cruz, T. Rajmankina, Trans. Met. Chem. 21 (1996) 11.
[38] (a) A. Smith, J.H.P. Utley, Chem. Commun. (1965) 427;
(b) H. Adkins, H.L. Leonradt, J. Am. Chem. Soc. 63 (1941) 1563.
[39] A.H. Jackson, A.E. Smith, J. Chem. Soc. (1964) 5510.
[40] (a) P. Laszlo (Ed.), Preparative Chemistry Using Supported Reagents, Academic Press, San Diego, CA, 1987;
(b) K. Smith (Ed.), Solid Supports and Catalysts in Organic Synthesis, Ellis Horwood, New York, 1992;
(c) J.H. Clark, Catalysis of Organic Reactions by Supported Inorganic Reagents, VCH, New York, 1994;
(d) G.W. Kabalka, R.M. Pagni, Tetrahedron 53 (1997) 7999;
(e) P.J. Kropp, G.W. Breton, J.D. Fields, J.C. Tung, B.R. Loomis, J. Am. Chem. Soc. 122 (2000) 4280.
[41] U.K. Singh, M.A. Vannice, J. Catal. 199 (2001) 73.
[42] (a) R. Wilczynski, W.A. Fordyce, J. Halpern, J. Am. Chem. Soc. 105 (1983) 2066;
(b) W.A. Fordyce, R. Wilczynski, J. Halpern, J. Organomet. Chem. 296 (1985) 115.
[43] C. Bianchini, K.G. Caulton, K. Folting, A. Meli, M. Peruzzini, A. Polo, F. Vizza, F. Zanobini, J. Am. Chem. Soc. 114 (1992) 7290.
[44] (a) C. Bianchini, K.G. Caulton, C. Chardon, M.-L. Doublet, O. Eisenstein, S.A. Jackson, T.J. Johnson, A. Meli, M. Peruzzini, W.E. Streib, F. Vizza, Organometallics 13 (1994) 2010;
(b) C. Bianchini, K.G. Caulton, C. Chardon, O. Eisenstein, K. Folting, T.J. Johnson, A. Meli, M. Peruzzini, D.J. Rauscher, W.E. Streib, F. Vizza, J. Am. Chem. Soc. 113 (1991) 5127.
[45] P.T. Suryawanshi, V.V. Mahajani, J. Chem. Tech. Biotechnol. 69 (1997) 154.
[46] R.L. Augustine, in: Heterogeneous Catalysis for the Synthetic Chemist, Dekker, New York, 1996, p. 403, Ch. 17.